

System size dependence of the K^*/K ratio at LHC energies

C. Le Roux^{1,*}, F. S. Navarra¹ and L. M. Abreu²

¹*Departamento de Física Nuclear, Instituto de Física, Universidade de São Paulo, Rua do Matão, 1371, CEP 05508-090, São Paulo, SP, Brasil*

²*Instituto de Física, Universidade Federal da Bahia, Campus Universitário de Ondina, 40170-115, Bahia, Brazil*

E-mail: chiara.roux@usp.br, navarra@if.usp.br, luciano.abreu@ufba.br

In the beginning of high energy heavy ion collisions, a deconfined phase of quarks and gluons (QGP) is formed. After the QGP, there is a hadron gas (HG) phase, which evolves until the final fluid freeze-out. The study of hadron resonances, such as the K^* , may give valuable information about the HG phase. In a recent work, we studied the K^* meson evolution in heavy ion collisions during the hadron gas phase. We used the production and absorption cross sections of the K^* and K mesons in a hadron gas, which were calculated in a previous work. We computed the time evolution of the K^* abundance and the K^*/K ratio during the hadron gas phase. Assuming a Bjorken type cooling and using an empirical relation between the freeze-out temperature and the central multiplicity density, we were able to write K^*/K as a function of $(dN/d\eta(\eta = 0))$. The obtained function is in very good agreement with recent experimental data. In this communication we review the main points of these works and expand the discussion.

*XV International Workshop on Hadron Physics (XV Hadron Physics) 13 - 17 September 2021
Online, hosted by Instituto Tecnológico de Aeronáutica, São José dos Campos, Brazil*

*Speaker

1. Introduction

In the beginning of high energy heavy ion collisions quark-gluon-plasma (QGP) is formed. It expands, cools down and quarks, antiquarks and gluons recombine to form hadrons (“hadronize”). After hadronization the system becomes a hot hadron gas in which inelastic reactions occur, changing the relative abundance of the hadrons. The system further expands and cools down until the thermal freeze-out, when all interactions cease and the hadronic multiplicities are frozen. The final yield of hadrons is thus influenced not only by their production rate at the quark-hadron transition point but also by the interactions that they undergo after hadronization, which might increase or decrease their abundances.

The K^* meson is a resonance and may change its abundance also by the strong decay $K^* \rightarrow K\pi$. This meson has a lifetime of 4 fm/c, smaller than the duration of the hadron gas phase, which is believed to be of the order of 10 fm/c. The K^* s which decay in the medium are lost and we may observe a reduction in the final yield of this resonance, which would then be attributed to the existence of the hadron gas phase. The hadron gas phase could be tested through the study of the abundances of such particles. This idea has been discussed in several publications [1, 2].

In the hadron gas formed in heavy ion collisions, the temperatures range from $\simeq 175$ MeV, where hadronization takes place, to $\simeq 100$ MeV, where kinetic freeze-out takes place. Hence the K^* s interact at low energies with light mesons and baryons. Although the coupling constants $BB'K^{(*)}$ (baryon-baryon-strange meson) are relatively small [3], it has been shown in [4] that the interaction cross sections are significant and the K^*N total cross section can be as large as 20 mb. On the other hand, in the relevant region of the phase space, the baryons are relatively rare. Therefore, in [2] we neglected K^* interactions with baryons. In [5] K^* interactions with light mesons were studied with effective Lagrangians. In a subsequent work [6] the cross sections for production and annihilation of K^* and K mesons were recalculated with the inclusion of new reaction mechanisms, such as anomalous parity vector-vector-pseudoscalar interactions and also the exchange of axial resonances in the s and t channels. In Refs. [7], it was shown that interaction terms with anomalous parity couplings have a strong impact on the corresponding cross sections. In [6] these interaction terms were found to be relevant also in the calculation of K^* absorption processes. The results in Ref. [6] show that the new mechanisms are rather significant, changing the cross sections up to one or two orders of magnitude.

In a previous work [2] we used the improved cross sections of [6] to calculate the K^*/K ratio as a function of the system size (represented by $dN/d\eta(\eta = 0)$). Our results were in very good agreement with experimental data published in [8]. In this contribution we review the main results found in [2] and expand the discussion.

2. Formalism

For our purposes the most relevant dynamical quantity is the thermally averaged cross section. For a process $a + b \rightarrow c + d$ it is defined as:

$$\langle \sigma_{ab \rightarrow cd} v_{ab} \rangle = \frac{1}{1 + \delta_{ab}} \frac{\int d^3 \vec{p}_a d^3 \vec{p}_b f_a(\vec{p}_a) f_b(\vec{p}_b) \sigma_{ab \rightarrow cd} v_{ab}}{\int d^3 \vec{p}_a d^3 \vec{p}_b f_a(\vec{p}_a) f_b(\vec{p}_b)}, \quad (1)$$

where v_{ab} is the relative velocity between the initial particles and $f_i(\vec{p}_i)$ is the thermal momentum distribution of particle i , which is given by a Bose-Einstein distribution. According to Refs. [5] and [6], the most relevant interactions of the K^* meson are: $K^*\rho \rightarrow K\pi$, $K^*\pi \rightarrow K\rho$ and $K^* \rightarrow K\pi$, as well as the respective inverse processes. Restricting ourselves to the processes above, the system of differential rate equations can be written as:

$$\frac{dN_{K^*}(\tau)}{d\tau} = \gamma_K N_K(\tau) - \gamma_{K^*} N_{K^*}(\tau), \quad \frac{dN_K(\tau)}{d\tau} = -\gamma_K N_K(\tau) + \gamma_{K^*} N_{K^*}(\tau), \quad (2)$$

where N_K and N_{K^*} are the abundances of K and K^* mesons respectively. They are functions of the proper time τ . The factors γ_K and γ_{K^*} depend on the interaction cross sections and the light meson densities in the following way:

$$\begin{aligned} \gamma_K &= \langle \sigma_{K\pi \rightarrow K^*\rho} v_{K\pi} \rangle n_\pi + \langle \sigma_{K\rho \rightarrow K^*\pi} v_{K\rho} \rangle n_\rho + \langle \sigma_{K\pi \rightarrow K^*} v_{K\pi} \rangle n_\pi, \\ \gamma_{K^*} &= \langle \sigma_{K^*\rho \rightarrow K\pi} v_{K^*\rho} \rangle n_\rho + \langle \sigma_{K^*\pi \rightarrow K\rho} v_{K^*\pi} \rangle n_\pi + \langle \Gamma_{K^*} \rangle. \end{aligned} \quad (3)$$

where n_i is the density of particles of species i in the hadron gas at proper time τ and $\langle \Gamma_{K^*} \rangle$ is the thermally averaged decay width of K^* (see [2] for details).

Once we define the temperature evolution (“cooling”) of the hadron gas $T(\tau)$ and the initial conditions $N_{K^*}(\tau_h)$ and $N_K(\tau_h)$, the system of differential equations (2) can be solved, yielding N_{K^*} , N_K and the ratio $R(\tau) = N_{K^*}/N_K = K^*/K$. We follow the time evolution of the abundances until the kinetic freeze-out of the gas, which is defined by the freeze-out temperature T_f and occurs at time τ_f . Assuming that the hadronic system undergoes a Bjorken-like expansion, we have the simple relation between temperature and time $T = T_h (\tau_h/\tau)^{1/3}$, where $T_h = 175$ MeV is the universal hadronization temperature discussed above and τ_h is the hadronization time, which may change from system to system. As it was pointed out long ago [9], the kinetic freeze-out temperature is not an universal constant. It depends on the size of the hadronic system and hence on the collision energy, on the mass number of the colliding nuclei and on the centrality of the collision. A recent blastwave fit analysis made by the ALICE Collaboration [10] has confirmed that the kinetic freeze-out temperature decreases with the system size, customarily associated to the multiplicity density of charged particles, $dN/d\eta$, measured at midrapidity.

3. Results and Discussion

We solve the equations (2) using as input the cross sections calculated in [5] and in [6]. The initial temperature is $T_h = 175$ MeV and the initial conditions are $K^*/K = 0.2, 0.5$ and 0.8 . The results are shown in Fig. 1. On the left (right) panel the inputs are from Ref. [5] ([6]). We observe that when there is no cooling the system evolves to an asymptotic state where the abundances become constant. When Bjorken cooling is included, the ratio K^*/K drops and at typical freeze-out times of 20 - 25 fm/c reaches 0.2 - 0.3. These numbers are close to the measured ones. This suggests that a cooling faster than Bjorken is probably incompatible with data. Another interesting aspect of the figure is that, even with cooling, after some time of evolution the K^*/K ratio becomes the same for all initial conditions. When there is no cooling the ratio shown on the left (with the inputs from [5]) is significantly smaller than the one on the right (with the inputs from [6]). At higher temperatures, with [6] the cross section for K^* production is bigger and so is the ratio R . It

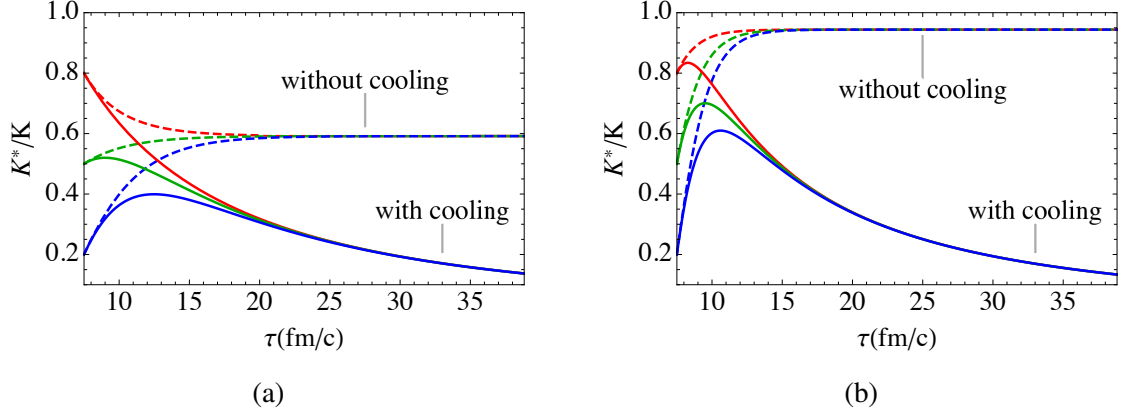


Figure 1: K^*/K ratio as a function of the proper time τ . Dashed lines correspond to the initial conditions 0.2, 0.5 and 0.8 and no cooling. Solid lines correspond to the initial conditions 0.2, 0.5 and 0.8 and cooling. a) Cross sections from S. H. Lee *et al* [5]. b) Cross sections from A. Martinez *et al* [6].

is also for this reason that on the right panel we observe a growth, in some cases very pronounced, of all lines at early times. In [6] all the cross sections are bigger, all the reactions happen faster and hence the system loses sooner the memory of the initial conditions (the three lines become a single line). Interestingly, at very long times in both cases (right and left panels) the ratio goes to the same value.

In order to compare our results with data, we will make use of the connection established in [10] between T_f and N . We fit the points presented in [10] with the form:

$$T_f = T_{f0} e^{-b N}, \quad (4)$$

where $T_{f0} = 132.5$ MeV and $b = 0.02$. The above expression is compared to the data points from [10] in Fig. 2a. To proceed further, we first choose the system under consideration, fixing N . This determines the freeze-out temperature, T_f , and the endpoint of the evolution, τ_f . Then, we read the ratio K^*/K from Fig. 1. Finally, we plot K^*/K as a function of N and compare the results with the data compilation published in [8]. The comparison is presented in Fig. 2b. As it can be seen in Fig. 1, the longer the hadronic system lasts, the smaller is the ratio R . Indeed, for each (increasing) value of N we stop the evolution at an (increasing) value of τ (which is τ_f) and read from Fig. 1a (decreasing) value of the ratio K^*/K . There is a strong correlation between Fig. 2a and Fig. 2b. A steeper function in the first figure implies a steeper function in the second. Interestingly, the data seem to exclude a flat horizontal line in Fig. 2a, i.e., a freeze-out temperature which is universal, independent of the system size.

To summarize: we have improved the treatment of the microscopic dynamics of K^* 's. We used all the relevant reaction cross sections involving K^* 's calculated in Ref. [6] as input in the evolution equations (2). We included cooling and the dependence of the freeze-out temperature on the system size. We obtained a very good description of the data published in [8] on $R = K^*/K$ as a function of $dN/d\eta(\eta = 0)$. In order to reproduce the features of Fig. 2b we need the three aspects of the process: i) dominance of the K^* absorption reactions; ii) cooling and iii) system size dependent freeze-out.

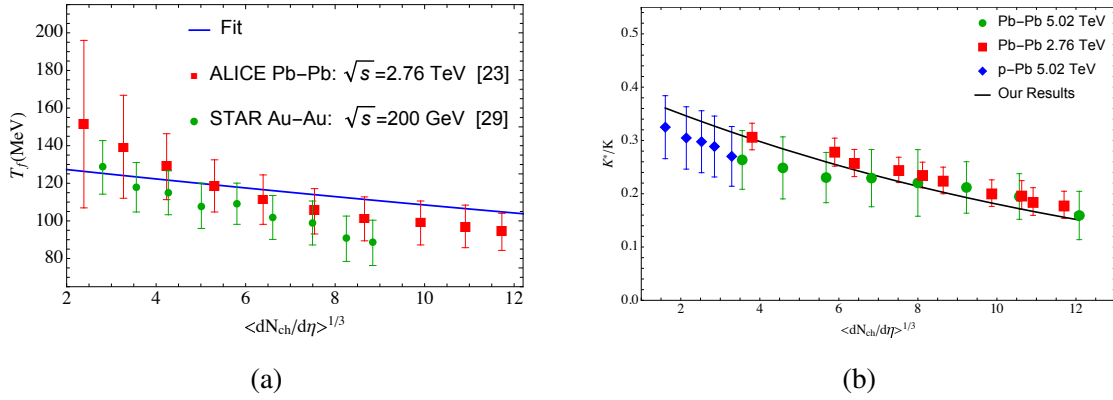


Figure 2: a) Freeze-out temperature as a function of $[dN/d\eta(\eta = 0)]^{1/3}$. The points are the result of the blastwave fits of data performed by the ALICE Collaboration [10]. The line represents the expression (4). b) K^*/K as a function of $[dN/d\eta(\eta = 0)]^{1/3}$. Data are from [8].

Acknowledgments

This work was partially financed by the Brazilian funding agencies CAPES and CNPq. We also would like to thank the INCT-FNA.

References

- [1] G. Torrieri and J. Rafelski, Phys. Lett. B **509**, 239 (2001).
- [2] C. Le Roux, F. S. Navarra and L. M. Abreu, Phys. Lett. B **817**, 136284 (2021). See references therein.
- [3] M. E. Bracco, F. S. Navarra and M. Nielsen, Phys. Lett. B **454**, 346 (1999).
- [4] K. P. Khemchandani, A. Martinez Torres, F. S. Navarra, M. Nielsen and L. Tolos, Phys. Rev. D **91**, 094008 (2015).
- [5] S. Cho and S. H. Lee, Phys. Rev. C **97**, 034908 (2018).
- [6] A. Martinez Torres, K. P. Khemchandani, L. M. Abreu, F. S. Navarra and M. Nielsen, Phys. Rev. D **97**, 056001 (2018).
- [7] Y. S. Oh, T. Song, and S. H. Lee, Phys. Rev. C **63**, 034901 (2001); F. Carvalho, F. O. Duraes, F. S. Navarra and M. Nielsen, Phys. Rev. C **72**, 024902 (2005).
- [8] S. Acharya *et al.* [ALICE Collaboration], Phys. Lett. B **802**, 135225 (2020).
- [9] Y. Hama and F. S. Navarra, Z. Phys. C **53**, 501 (1992).
- [10] B. Abelev *et al.* [ALICE Collaboration], Phys. Rev. C **88**, 044910 (2013).